PERGAMON

Journal of Structural Geology 21 (1999) 751–767

JOURNAL OF STRUCTURAL GEOLOGY

Deformation-induced inverted metamorphic field gradients: an example from the southeastern Canadian Cordillera

H. Daniel Gibson[a,*], Richard L. Brown[a], Randall R. Parrish[b]

[a]*Ottawa-Carleton Geoscience Centre and Department of Earth Sciences, Carleton University, Ottawa, Ontario, Canada K1S 5B6*
[b]*Department of Geology, University of Leicester and NERC Isotope Geosciences Centre, British Geological Survey, Keyworth, Nottinghamshire, NG12 5GG, UK*

Received 2 July 1998; accepted 11 February 1999

Abstract

Exhumed middle crustal rocks of the hinterland of the southeastern Canadian Cordillera were deformed and metamorphosed during Mesozoic and Tertiary progressive crustal thickening. High structural levels were transported to the northeast relative to lower levels through a combination of thrusting and ductile non-coaxial flow. Progressive growth of the orogen and advance of hinterland rocks toward the foreland are revealed through analysis of diachronous metamorphism and associated deformation. At the deepest exposed level, allochthonous rocks of the orogen (Selkirk allochthon) structurally overlie Early Proterozoic basement and younger cover rocks (Monashee complex) that are correlated with autochthonous North American crust underlying the eastern Foreland Belt. The crustal zone, which marks the boundary between the Selkirk allochthon and Monashee complex, exhibits an inverted metamorphic field gradient. New data presented in this paper refute previous interpretations, which asserted that the metamorphic inversion is a result of the downward transfer of heat from the allochthon to the underlying Monashee complex. Rather, the inversion is attributed to synmetamorphic non-coaxial progressive deformation. A model is proposed in which substantial northeastward directed shear strain and attendant attenuation led to lateral transfer of rocks thereby preserving evidence of strongly diachronous deformation and an apparent inverted metamorphism.

1. Introduction

Inverted metamorphic isograds are common features in the footwalls of crustal-scale thrust sheets; understanding the mechanisms responsible for their development is essential for thermotectonic modeling. Some explanations for inversion argue for transmission of heat into the footwall from above. These include mechanisms such as shear heating along thrust faults (e.g. England and Molnar, 1993) and/or heat transfer to a cool footwall from a hot overlying thrust sheet (e.g. Le Fort, 1975; Royden, 1993; Ruppel and Hodges, 1994) causing inversion of thermal gradients with an upward decrease in metamorphic pressures resulting in the inversion of metamorphic gradients (e.g. Hubbard, 1989; England and Molnar, 1993; Royden, 1993). Alternatively, inversion may be the result of mechanical repositioning of metamorphic isograds. This could involve folding of pre-existing isograds (e.g. Tilley, 1925; Bhattacharya and Das, 1983; Searle et al., 1992), post-metamorphic thrust stacking of isograds from different structural levels (e.g. Bordet, 1961; Treloar et al., 1989), displacement along shear zones (e.g. Brunel and Kienast, 1986; Jamieson, 1986; Reddy et al., 1993; Hubbard, 1996), or synmetamorphic ductile inversion by progressive shear strain of diachronous isograds (e.g. Grujic et al., 1996; Jamieson et al., 1996).

Much attention regarding this issue has been focused on the Main Central thrust zone (MCT) of the Himalayas (e.g. Le Fort, 1986; England and Molnar, 1993; Royden, 1993; Ruppel and Hodges, 1994; Grujic

* Corresponding author.
E-mail address: dngibson@ccs.carleton.ca (H. D. Gibson)

0191-8141/99/$ - see front matter
PII: S0191-8141(99)00051-6

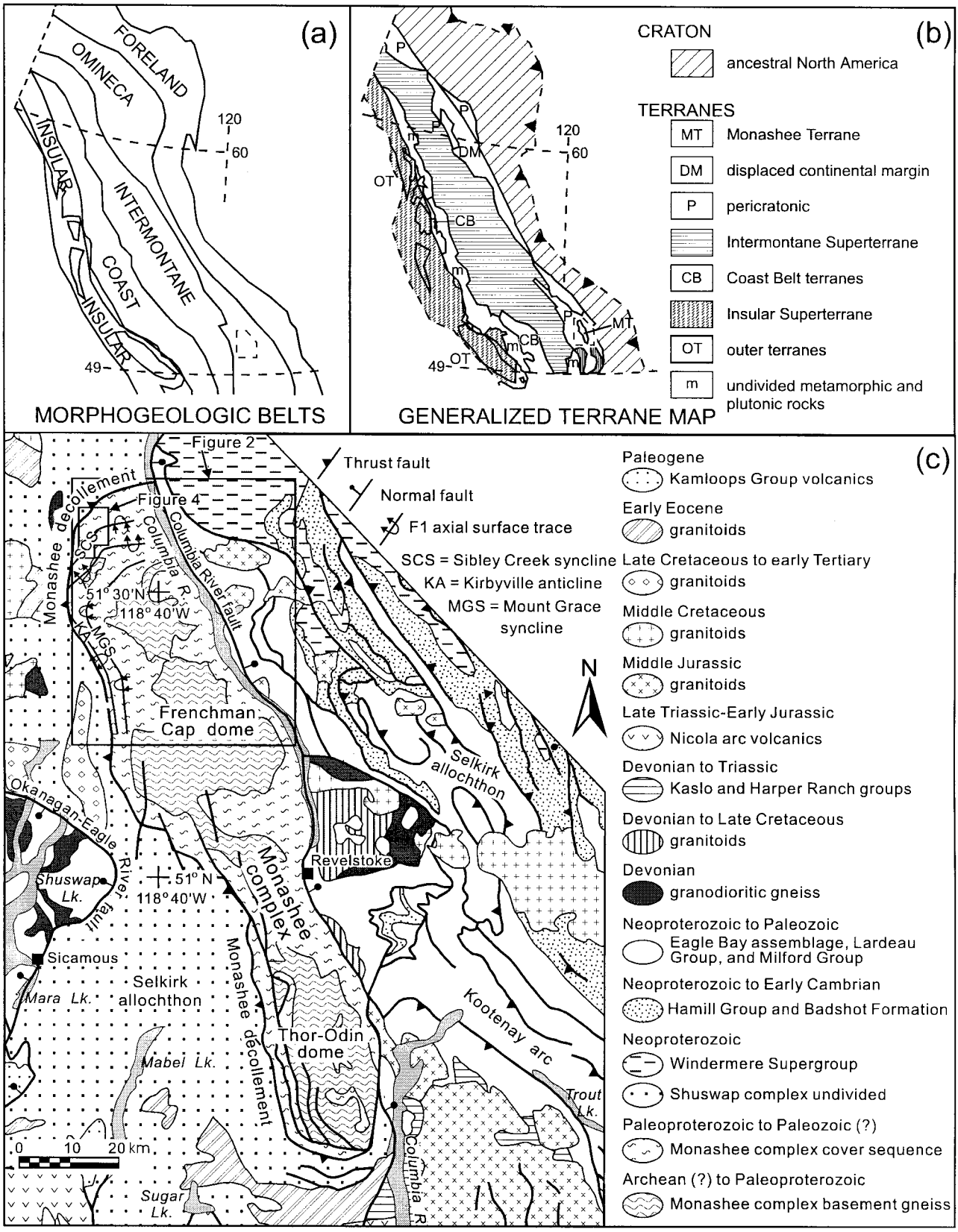

Fig. 1. (a and b) Morphogeologic belts and terranes of the Canadian Cordillera, modified from Wheeler and McFeely (1991). Box outlined within (a) delineates the map location for (c) within British Columbia and the Omineca Belt. (c) Tectonic map of southeastern Omineca belt, located in the hinterland of the Canadian Cordillera (modified from Scammell and Brown, 1990; Wheeler and McFeely, 1991) showing the footwall lithologies of the Monashee complex, surrounded by the hanging wall lithologies of the Selkirk allochthon. The ages of map units, where known, are provided.

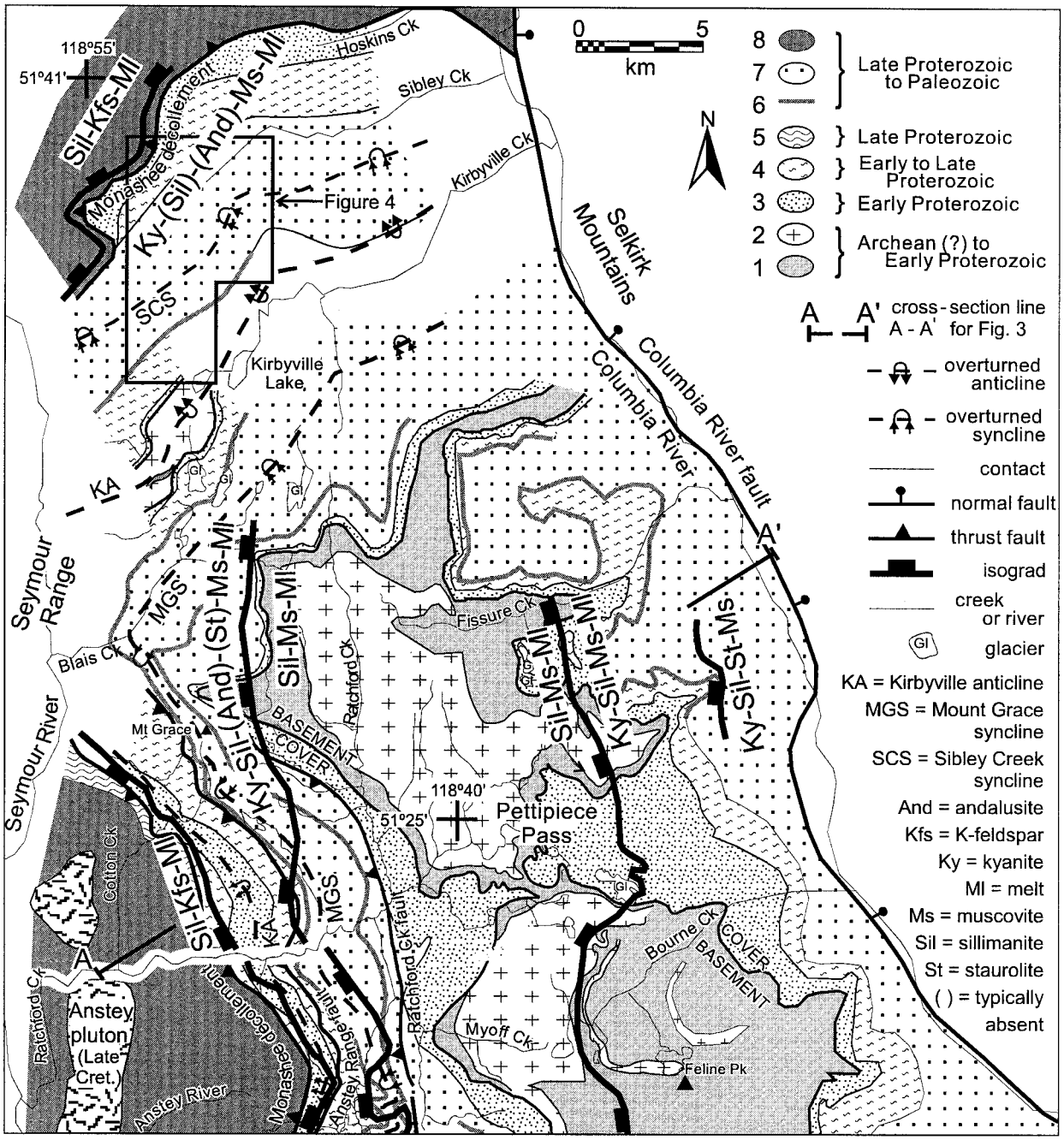

Fig. 2. Generalized geologic compilation map of Frenchman Cap dome, modified from Journeay (1986, 1991) and Brown and Journeay (1987). Box inset outlines field area for this study. Lithologies of Frenchman Cap dome are as follows. Monashee core gneisses: 1 = Bt–Hbl paragneiss, Bt–Qtz–Fsp paragneiss, amphibolite, pelitic and semi-pelitic schist; 2 = granitic to tonalitic orthogneiss, pegmatite, amphibolitic gneiss. Monashee cover gneisses: 3 = (lower assemblage) quartzite, pelitic and semi-pelitic schist; 4 = (lower and middle assemblage) quartzite, pelitic and semi-pelitic schist, minor marble; 5 = syenitic and granitic orthogneiss; 6 = (middle assemblage) white marble with a carbonatite horizon occurring a few metres below and the Pb–Zn 'Cotton belt' horizon occurring a few metres above; 7 = (upper assemblage) pelitic and semi-pelitic schist, quartzite, amphibolite, calc-silicate gneiss. Selkirk allochthon: 8 = Bt–Qtz–Fsp–paragneiss, quartzite, amphibolite, pelitic and semi-pelitic schist, abundant pegmatite.

et al., 1996; Hubbard, 1996; Jamieson et al., 1996). A large quantity of stratigraphic, structural, metamorphic, and chronologic data have been collected, but there remains little agreement concerning the mechanisms responsible for the inversion. Another example of apparent metamorphic inversion is found in the southern Canadian Cordillera in a diffuse zone that straddles the boundary between the Selkirk allochthon and its immediate footwall. This footwall is the Monashee complex, which is exposed in a tectonic

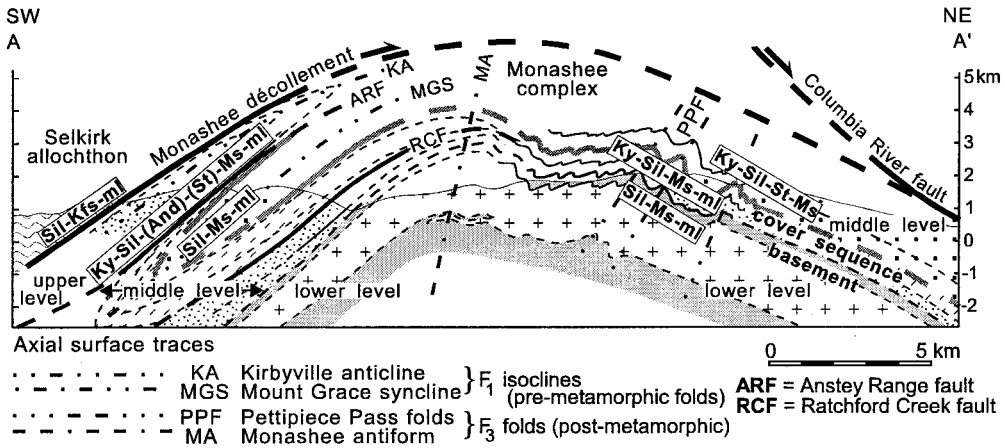

Fig. 3. Cross-section of northern Frenchman Cap dome near Pettipiece Pass showing approximate structural position of the metamorphic mineral assemblages in pelitic schists of the cover sequence (modified after Crowley, 1997, Journeay, 1986 and references therein). Crowley (written communication, 1998) interpreted the metamorphic assemblages for this part of the complex to reflect an inverted metamorphic sequence at the highest structural levels above the staurolite-out isograd and a normal hot-side-down metamorphic sequence below it. Assemblages in the basement are not shown because it is uncertain whether the minerals grew during Proterozoic or early Tertiary metamorphism. See Fig. 2 for mineral abbreviations, legend and location of line of cross-section.

window through the basal zone of the thrust sheet (Figs. 1c–3) (Brown, 1980; Read and Brown, 1981; Journeay, 1986). Metamorphism within the region was complex and quite likely involved multiple episodes of mineral growth, as demonstrated by Journeay (1986, 1991) and Scammell (1986). Both authors describe in detail complicated textural relationships among mineral phases within a given assemblage and have assigned at least two episodes of prograde metamorphism. In this study, we do not refute these findings but do focus on the most important aspect of the two mentioned studies, i.e. that within the uppermost footwall and immediate hanging wall there is an apparent inverted metamorphic field gradient. This conclusion is based primarily on the observation (by all authors) that at the highest structural level there is a zone of sillimanite–K-feldspar-melt that is structurally underlain by a zone of kyanite plus stable muscovite (Figs. 2–4). At deeper structural levels towards the core of the complex, the metamorphic assemblages appear to exhibit a normal gradient as demonstrated in Fig. 3. However, at this depth it becomes difficult to separate out the effects of Cordilleran metamorphism from a Precambrian metamorphism that has affected basement rocks (Armstrong et al., 1991; Crowley, 1999). Sillimanite and andalusite within the latter zone have only a localized occurrence and are typically absent.

Both Journeay (1986) and Scammell (1986) attributed the inversion to heat transfer from the Selkirk allochthon. Parrish (1995) supported this conclusion on the basis of geochronologic data. The purpose of this communication is to present new structural and geochronologic data from the Monashee complex that appear to be incompatible with such a heat transfer model. To reconcile these new results with previous data and interpretations, we propose a model that attributes the inversion primarily to diachronous heating during burial of the footwall and to progressive ductile deformation resulting in the mechanical inversion of isograds. This model does not exclude the probability of some degree of downward heat transmission from the allochthon to the complex but does imply that mechanical inversion of isograds was the dominant process in this part of the footwall.

2. Geological setting

The Monashee complex, exposed through a structural window within the metamorphic hinterland of the southern Canadian Cordillera (Figs. 1–3) is an exhumed basement complex of middle crustal rocks, interpreted to be an inlier of the North American craton (Armstrong et al., 1991; Parrish, 1995 and references therein). The Monashee complex consists of two distinct polydeformed and metamorphosed assemblages. Coring the complex are Early Proterozoic crystalline orthogneiss and paragneiss rocks of North American cratonic affinity (Armstrong et al., 1991); these rocks are unconformably overlain by the Monashee cover sequence, a 2–3 km thick, laterally extensive assemblage of metasedimentary siliciclastic and carbonate rocks interlayered with meta-igneous rocks (Wheeler, 1965; Scammell and Brown, 1990 and references therein). The cover sequence is thought to have been deposited on the stable western continental

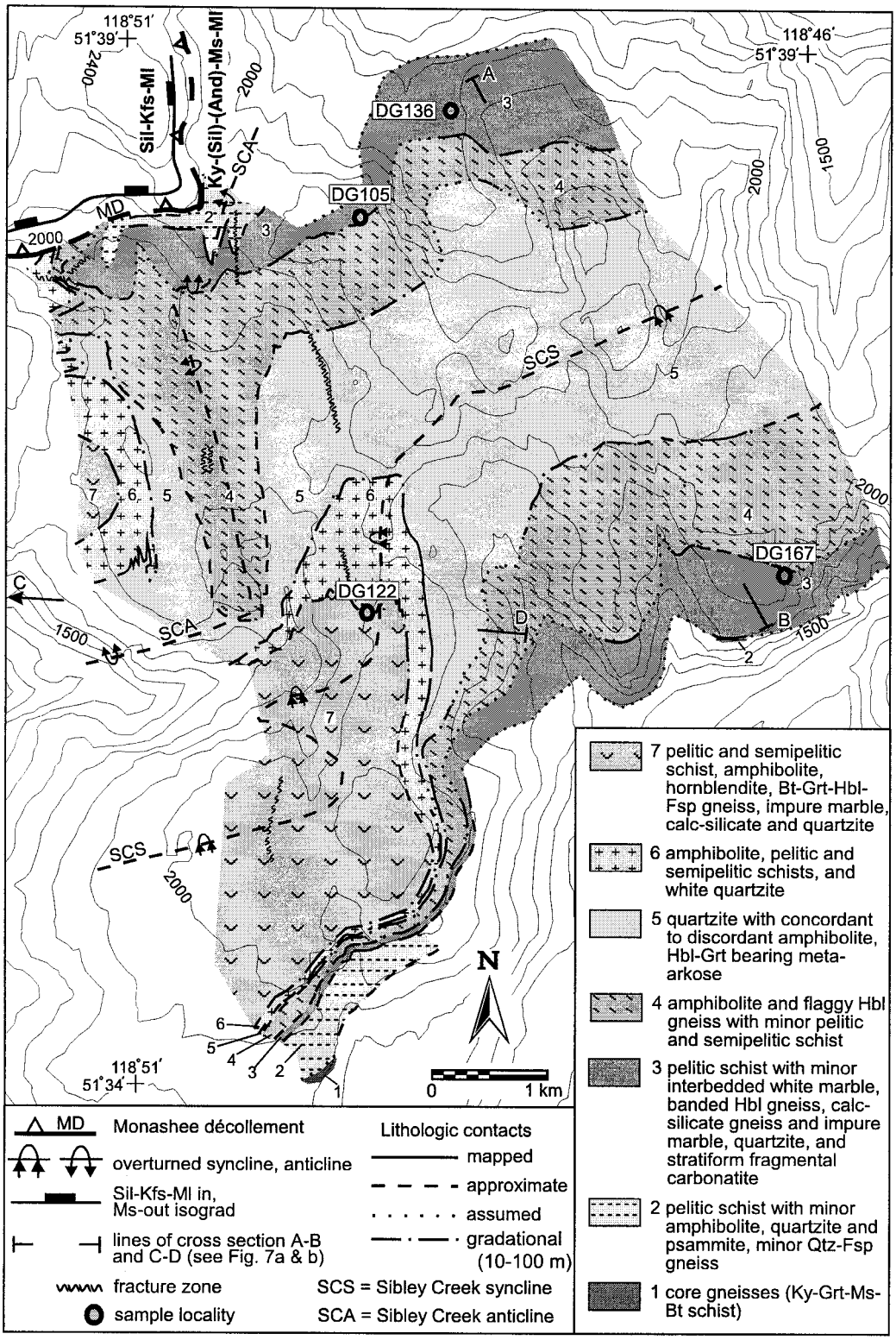

Fig. 4. Simplified lithologic compilation map of northern Frenchman Cap dome incorporating detailed mapping (1:15 000) of Scammell (1986) and this study. Sample locations (e.g. DG105) for this study's geochronology are included. A–B and C–D indicate cross-section lines for Fig. 7(a) and (b). Contour interval is every 100 m.

margin of paleo-North America (Scammell and Brown, 1990).

Bounding the Monashee complex to the north, west, and south is a crustal-scale northeastward-directed ductile shear zone termed the Monashee décollement (Read and Brown, 1981; Journeay, 1986), which is thought to be the western continuation of the sole thrust of the Foreland Belt (Fig. 1a; Brown et al., 1992; Cook et al., 1992). The shear zone separates the basement and cover sequences of the complex from the hanging-wall rocks of the Selkirk allochthon (Figs. 1c–3). The eastern limit of the complex is defined by the Columbia River fault (CRF) (Figs. 1c and 2), an east-dipping Eocene normal-sense shear zone partly responsible for the tectonic unloading of the complex (Journeay and Brown, 1986; Parrish et al., 1988; Carr, 1991; Johnson and Brown, 1996).

Interpretation of the tectonic history of the complex has evolved substantially over the past decade. It was generally agreed that the complex was buried during crustal thickening associated with the Cordilleran orogeny, but the timing of initial burial at pre-peak-metamorphic conditions was uncertain. Brown (1980) first suggested that burial occurred as early as the Jurassic. Journeay (1986) and Brown et al. (1986) modified this idea by proposing a duplex model of crustal thickening of the complex beneath the Selkirk allochthon. This model implied that eastwardly displacement began in the Jurassic and progressed into the Tertiary. The complex was thought by Brown and Journeay (1987) to have been exhumed initially during the late stages of compression with final exhumation occurring as the result of extension and tectonic denudation in the Eocene.

Parrish (1995) reinterpreted the tectonic history of the Monashee complex based on new geochronologic data. He argued that the complex is autochthonous and was not deeply buried until the Paleocene, on the basis of early Tertiary metamorphic ages in the complex. Parrish proposed that burial of the complex beneath the hot Selkirk allochthon was rapid and was quickly followed by exhumation in the Paleocene to Eocene, which allowed for the inversion and preservation of the present-day metamorphic isograds.

3. Structural setting of the northern Monashee complex

The northwest portion of the Monashee complex is dominated by a regional-scale isoclinal fold system that includes, from south to north, the Mount Grace syncline, the Kirbyville anticline, and the Sibley Creek syncline together with a locally preserved complementary anticline (Figs. 1, 2 and 4). Axial surfaces of these folds dip moderately away from the complex toward the northwest and southwest (Brown, 1980; Höy and Brown, 1980). Both the basement and cover gneiss sequences of the complex are involved in these structures which form kilometre-scale, eastward vergent isoclinal nappes. These structures are thought to be coeval with the earliest stages of Cordilleran deformation recorded in the complex (Journeay, 1986; Scammell, 1986) and are therefore important to the overall understanding of its thermotectonic evolution.

This study is focused on the northern flank of the Monashee complex (Fig. 4) where the Sibley Creek syncline and its associated structures are found. Many of the structural elements described herein have been previously documented by Scammell (1986). Structural data gathered during this study are presented in the structural map of Fig. 5. Ascribing of structures to a 'generation' has been based on superposition of one generation upon the other as observed at outcrop and hand specimen-scale. As such, 'generations' have geometric and sequential significance, but time correlations (at the regional scale in particular) are not implied. Indeed, data presented here demonstrate that 'generations' are diachronous.

The Sibley Creek syncline is a first generation structure (F_1), a pre- to early-metamorphic (Journeay, 1986; Scammell, 1986), kilometre-scale, overturned, and non-planar fold that controls map-scale geometry (Fig. 4). Its axial surface is periclinal and moderately dipping ($\sim$20–30°), and the hinge line plunges shallowly at $\sim$10–25° towards the west-southwest (Scammell, 1986). The trend and plunge of the hinge line are based on stereonet calculations using strike and dip measurements of compositional layering in opposing limbs (Scammell, 1986) and direct measurement of hinge lines of minor folds (this study, Fig. 6c). Journeay (1986) also measured shallow south-plunging hinge lines for this generation of folding along the western flank of the complex. The mechanism that caused the variation in the orientation of these hinge lines is discussed below. The Sibley Creek syncline is well-defined by a distinctive lithology that can be walked around major closures. Stratigraphic facing directions have been determined from cross-bedding found in competent quartzites in the hinge zone of the syncline (this study; Scammell and Brown, 1990).

The Sibley Creek syncline has highly attenuated limbs that thicken dramatically towards its hinge (Fig. 4). This is especially true for unit 5 quartzite, which increases from less than 1 m in thickness in the lower limb to greater than 1 km in the hinge zone, suggesting that transposition occurred during folding causing lithologic layering to become subparallel to the axial plane of the syncline. The trend of the hinge line for the syncline varies between a shallow western plunge in the east and a southwestern plunge in the west (Scammell, 1986; Fig. 6c). This is likely attributable to subsequent doming of the complex, bending the syn-

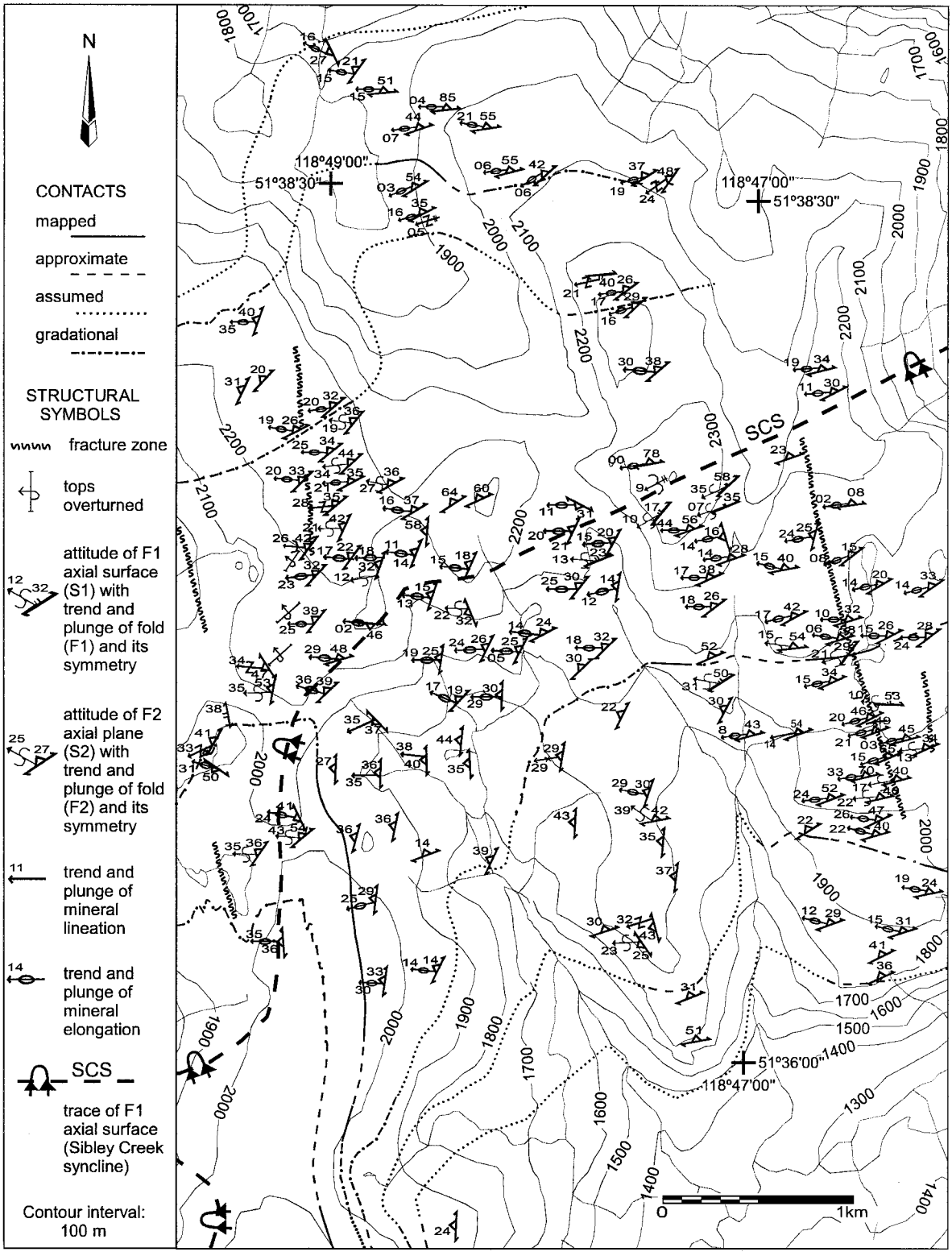

Fig. 5. Structural map of northern Monashee complex, within the southeastern Canadian Cordillera. Pertinent structural data collected during the course of this study are included.

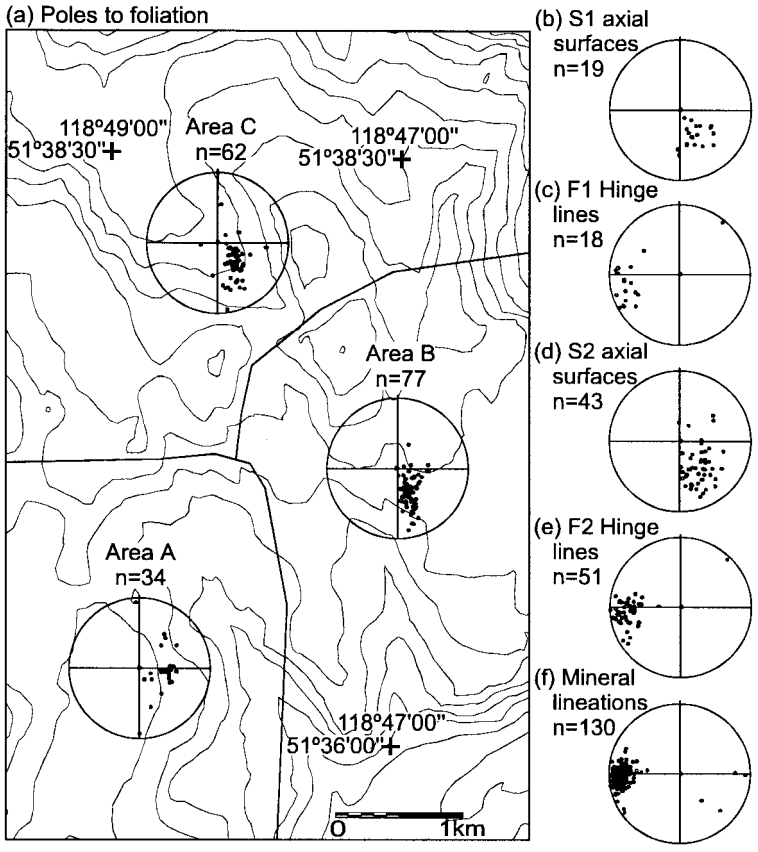

Fig. 6. Poles to the axial surfaces for F_1 (S_1) and F_2 (S_2) throughout total field area and their respective hinge lines; note that mineral lineations are colinear with the hinge lines. Poles to transposition foliation are separated into three domains (A, B, and C) within the map.

cline around the northwest corner of the dome (Brown, 1980). The interpretation is also supported by the change in direction of the axial surface trace of the syncline from east–west in the east to northeast–southwest in the west (Figs. 4 and 5).

The Sibley Creek syncline and its related macroscopic folds (i.e. Mount Grace syncline, Kirbyville anticline) do not appear on the eastern side of the complex (Psutka, 1978; Höy and Brown, 1980); thus the development of overturned stratigraphy due to this generation of folding is restricted to the west flank of the complex. The proximity of these structures to the basal zone of the Selkirk allochthon suggests that their formation is a result of its emplacement.

In the hinge zone of the Sibley Creek syncline, parasitic folds and associated fabrics are sparse and are only clearly identified in the eastern portion of the field area in competent lithologies such as the unit 5 quartzite (Fig. 4). The minor folds are close to tight and vary between Class 1C and Class 2 similar folds (Ramsay and Huber, 1987). They are usually 1–2 m in scale, symmetric in the hinge zone to strongly asymmetric towards the limbs. Hinges plunge shallowly to the west and west-southwest, and axial planes dip moderately to the north and northwest. In the highly attenuated limbs of the Sibley Creek syncline these associated minor structures become completely isoclinal and boudinaged and are rarely preserved.

Penetrative second generation structures (F_2) dominate the deformation observed at the outcrop scale where they overprint F_1 structures. F_2 folds locally vary between northward and southward vergent but do not systematically change vergence across the hinge of the Sibley Creek syncline (Fig. 5). They are asymmetrical, tight to isoclinal, overturned, reclined, and locally disharmonic. The axial planes (S_2) dip moderately to the west and northwest, parallel to the penetrative foliation found throughout most of the field area (Figs. 5 and 6d), and for the most part are parallel to sub-parallel to the compositional layering. Stereonets in Fig. 6 (e) and (f) demonstrate that the hinges of F_2 plunge shallowly to the west and are colinear with a regional lineation defined by elongated quartz and feldspar aggregates and by the alignment of prismatic metamorphic minerals such as kyanite, sillimanite, and amphibole (Journeay, 1986; Scammell, 1986).

The geometry of these F_2 folds indicates that they are products of both passive and flexural flow folding (Scammell, 1986), suggesting high temperatures during

Table 1
Geochronology sample information

Sample	Lithology and location[a]	Mineralogy[b]	Textures/Fabrics in hand sample and thin section	$^{208}Pb/^{232}Th$ age (Ma)
DG105 (m.g.)[c]	Unit 3 pelitic schist; elevation 2242 m; upper overturned limb of SCS[d]; ~510 m below MD[d] surface	Qtz, Pl, Ms, Bt, Grt, Ky, Mnz, Rt, Opq	Penetrative foliation in hand sample and thin section, designated S_2, defined by alignment of metamorphic minerals (e.g. Ky, Bt) axial planar to F_2; some Ky and Bt are deformed by F_2 (e.g. kinked) while others cross-cut the fabric; F_2 is interpreted to have been coeval with peak metamorphism	77.7±0.3 to 66.8±0.3
DG136 (s.g.)	Unit 3 pelitic schist; elevation 1880 m; upper overturned limb of SCS; ~600 m below MD surface	Qtz, Pl, Kfs, Bt, Ms, Grt, Ky, Sil, Mnz, Rt, Opq	Similar fabric to DG105; many grains are randomly orientated, and serrated boundaries between Pl grains suggest dynamic recrystallization; peak minerals also show evidence of strong deformation in the form of subgrain boundaries, undulatory extinction, kinks; Sil (fibrolite) grew at the expense of Bt and Ky	73.6±0.3 to 63.4±0.3
DG122 (m.g.)	Unit 3 pelitic schist; elevation 1990 m; upper overturned limb of SCS near hinge; ~2200 m below MD surface	Qtz, Pl, Ms, Bt, Grt, Ky, Mnz, Rt, Opq	Strong alignment of metamorphic minerals parallel to S_2; most have undulatory extinction and subgrain boundaries; brittle post-S_2 deformation observed in the form of pulled apart Ky and Bt, and discrete shear bands cutting S_2 displaying sinistral tops-to-the-west sense of movement	61.8±0.3 to 57.6±0.2
DG167 (m.g.)	Unit 3 pelitic schist; elevation 1950 m; lower upright limb of SCS; ~3010 m below MD surface	Qtz, Pl, Ms, Bt, Grt, Ky, Sil, Mnz, Rt, Opq	Very similar textures and fabrics to DG122, with the exception that there is more Ms and Sil (fibrolite) in this sample; both DG167 and DG122 appear to be not as annealed as the upper two samples, possibly due to their more limited peak thermal histories relative to deformation	59.9±0.3 to 59.4±0.20

[a] Elevations are taken above mean sea level.
[b] abbreviations for minerals taken from Kretz (1983).
[c] (m.g) and (s.g.) indicate multiple grain and single grain analyses for the sample.
[d] SCS = Sibley Creek syncline; MD = Monashee décollement.

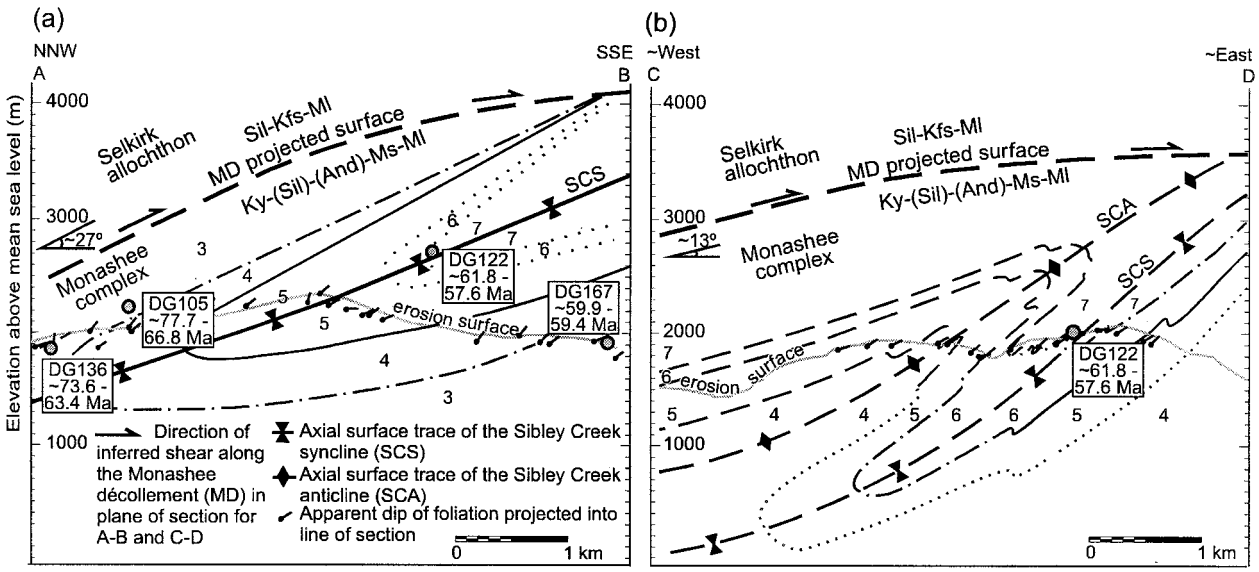

Fig. 7. Generalized cross-sections of (a) the Sibley Creek syncline (SCS) and (b) the Sibley Creek anticline (SCA) constructed using best fit between orthographic projection and projection of data off line of section along strike or down dip, and plotting apparent dip. Geochronology sample localities (with $^{208}Pb/^{232}Th$ ages) have also been projected into section. Lines of section (A–B, C–D) are constructed at an acute angle to each other using data from this study and from that published by Scammell (1986); the lines are chosen to be approximately perpendicular to the trend of the SCS and SCA axial surface traces. Scales are approximately the same. Location of lines of section A–B and C–D and descriptions of lithologic units (i.e. 3 through 7) are found in Fig. 4.

their formation. This is confirmed by the observations at the outcrop, hand sample, and thin section-scale, which indicate that the growth of peak mineral assemblages both pre-dated and outlasted the F_2 fabrics. These observations and interpretations are supported by those made by Journeay (1986), who attributed the colinearity between hinge-line orientation of F_2 folds and the regional trend of mineral lineations to high-temperature passive rotation of fold hinges during non-coaxial flow associated with the east-northeast-directed overthrusting of the Selkirk allochthon. If so, it is apparent that the Sibley Creek syncline and its associated fabrics were significantly modified during generation of F_2 structures.

Within the study area no significant ductile structures have been recognized that post-date F_2. Regionally, however, post-F_2 deformation includes folding that is particularly well-developed along the eastern flank of the complex (cf. Brown and Psutka, 1979; Journeay, 1986). Large-scale open folds are also recognized and are thought to be related to the formation of the structural dome present in the northern part of the complex. Late structures in the vicinity of the Sibley Creek syncline consist of brittle north-trending and generally steeply dipping faults and fractures with minor displacements. These structures are thought to be associated with the Eocene extensional denudation of the complex, which was facilitated by normal-sense shearing along the Columbia River and Okanagan–Eagle River fault systems (Journeay, 1986; Parrish et al., 1988; Parrish, 1995; Johnson and Brown, 1996). Although most of these late features appear to be brittle in this part of the complex, to the west near the base of the Selkirk allochthon, Journeay (1986) described discrete west-dipping ductile normal-sense shear zones that are most likely also related to regional Eocene extension.

4. Timing constraints on deformation and metamorphism

4.1. Summary of geochronology

Dual Pb/U and $^{208}Pb/^{232}Th$ chronometry was carried out on monazite and zircon from six localities. Analytical data and interpretations made with regard to all aspects of the geochronology (e.g. mineral ages, timing of peak metamorphism, U–Th–Pb systematics) are presented in detail in Gibson (1997) and Gibson and Parrish, (in review). An overview of the pertinent information (location, mineralogy, textures and fabrics, $^{208}Pb/^{232}Th$ ages) regarding the rocks sampled for geochronologic analyses is provided in Table 1.

The $^{208}Pb/^{232}Th$ ages for this study are interpreted to be the most accurate approximation of the time of crystallization because the $^{208}Pb/^{232}Th$ isotopic system has proven to be more robust than the Pb/U system. The $^{208}Pb/^{232}Th$ isotopic system does not appear to be affected by troublesome complexities such as unsupported ^{206}Pb or U loss that have been demonstrated to

affect the Pb/U system (Keppler and Wyllie, 1990; Barth et al., 1994; Gibson, 1997; Gibson and Parrish, in review). Furthermore, all $^{208}Pb/^{232}Th$ ages are concordant (cf. Gibson and Parrish, in review). Thus, the ages referred to are those produced using $^{208}Pb/^{232}Th$ chronometry. Of particular significance are 16 monazite fractions extracted from four pelitic schist samples containing peak-metamorphic mineral assemblages of kyanite ± sillimanite, garnet, biotite ± muscovite, quartz, plagioclase ± K-feldspar. These samples were taken from systematically deeper structural levels beneath the Monashee décollement (Figs. 7a,b and 8). Additionally, three of the four pelitic samples were taken from the same lithologic unit which occurs in both the upper and lower limbs of the Sibley Creek syncline (unit 3 pelitic schist, Fig. 4). These data enable examination of the relative timing of deformation and metamorphism with increasing depth. The zircon Pb/U ages for this study (one sample) agree well with the monazite data but are not included in this communication because their ages from the preferred $^{208}Pb/^{232}Th$ isotopic system included very large errors resulting from uncertainties introduced by the common Pb correction due to low concentrations of radiogenic ^{208}Pb. For a more detailed examination of the zircon data, readers are referred to Gibson (1997) and Gibson and Parrish, in review.

The monazites described herein have been determined to be metamorphic based on morphology and textural evidence observed in thin section analyses (Table 1), which demonstrated an intimate intergrowth of monazite with peak-metamorphic minerals in all samples (e.g. Fig. 9). Zoning was not observed in any of the monazites analysed when examined using a polarizing microscope, and therefore, they were interpreted not to have inherited older cores representing an earlier metamorphic event. Inheritance cannot be completely ruled out without conducting a more detailed micro-analytical examination (e.g. S.E.M., micro-probe, SHRIMP) in a follow-up study. However, based on the available data from this study (cf. Gibson, 1997; Gibson and Parrish, in review) and on compelling evidence presented by Parrish (1995), Crowley (1997), and Crowley and Parrish (in press) in a study further south in the complex within rocks of similar composition and metamorphic grade, we interpret the monazite as having grown during a diachronous metamorphic event beginning in the Late Cretaceous.

Additionally, the U–Th–Pb ages produced are considered to represent the timing of monazite crystallization during high-temperature (minimum $>500°C$, Smith and Barreiro, 1990) prograde metamorphism as opposed to the time when the monazites cooled through their closure temperature (Dodson, 1973). This is based partly on the results described below but also on new data presented by Spear and Parrish (1996) which suggest that the monazite closure temperature is $>750°C$. Although the peak-metamorphic temperatures for this area are not well constrained, plotting of the peak-metamorphic assemblages on a petrogenetic grid (Spear, 1993) suggests that temperatures did not exceed 700°C (cf. Scammell, 1986). Monazite growth during retrograde cooling of the complex is considered unlikely for two reasons: (1) There is no textural evidence in thin section that supports this notion; (2) based on palinspastic reconstructions and post-thermal peak cooling histories gleaned from accessory minerals (e.g. titanite, hornblende, muscovite, biotite) other studies in and around the complex have concluded that immediately following the culmination of tectonic burial (Late Cretaceous to Paleocene) the complex was rapidly exhumed (e.g. Parrish, 1995 and references therein; Johnson and Brown, 1996; Crowley, 1997). Accordingly, peak mineral assemblages are thought to have quenched before they had a chance to re-equilibrate at lower metamorphic grades.

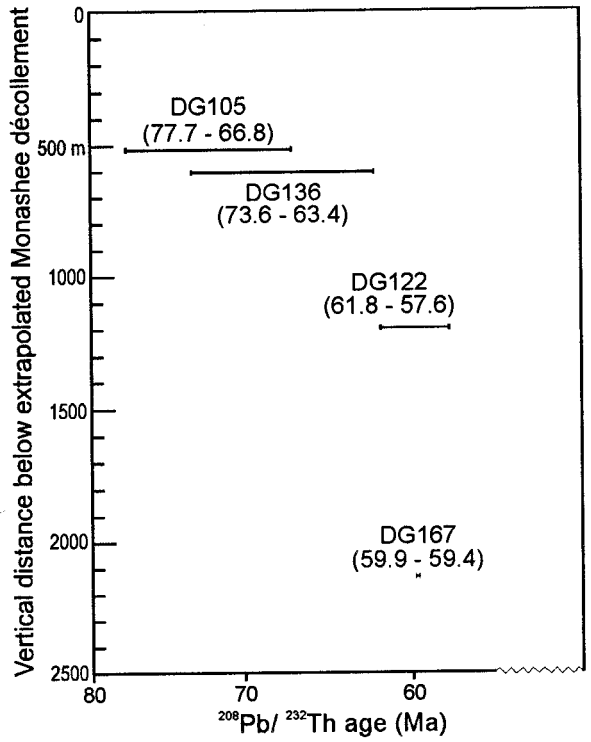

Fig. 8. Plot of age vs depth of sample below Monashee décollement. Note the downward younging and decrease in spread of metamorphic ages.

4.2. Sample DG105, unit 3, highest structural level, ~510 m below the Monashee décollement

Sample DG105 was taken from pelitic schist of unit

3, found within the upper, overturned limb of the Sibley Creek syncline (Figs. 4 and 7a). DG105 represents the highest structural level of all the analyses performed in this study (Fig. 8) and the sampling closest to the Monashee décollement of all rocks taken from the Monashee complex. The $^{208}Pb/^{232}Th$ ages for this sample range from 77.7 ± 0.3 to 66.8 ± 0.3 Ma, which is interpreted to be the minimum age range of prograde metamorphism and deformation (F_2) at this level based on textural and fabric relationships observed in thin section and hand sample (Table 1). These monazites are interpreted to have suffered noticeable amounts of U loss (~0.5–7%), based on discrepancies found in the U–Th–Pb isotopic data and the pattern of U–Th–Pb data in concordia diagrams (Gibson, 1997; Gibson and Parrish, in review). Therefore, monazite crystals in this sample are interpreted to have grown during a thermal history which involved a prolonged duration of elevated temperatures (at least as long as the range of isotopic ages) accompanied by deformation. The isotopic age for an individual crystal is inferred to be the cumulative average of variable contributions from older through younger monazite growth in this period of time (i.e. 77.7 Ma through 66.8 Ma).

4.3. Sample DG136, unit 3, ~600 m below the Monashee décollement

This sample was also taken from unit 3 within the upper, overturned limb of the Sibley Creek syncline but at a slightly lower structural level than DG105 (Figs. 4, 7 and 8). The $^{208}Pb/^{232}Th$ ages, ranging from 73.6 ± 0.3 to 63.4 ± 0.3 Ma, are similar to those produced for DG105 and are interpreted to be a minimum duration for prograde metamorphism and deformation (F_2), consistent with thin section and hand sample analysis. As for DG105, the interpreted environment was one of prolonged peak thermal conditions at this level. Additionally, U loss (~3.6–5.0%) is interpreted to be significant for all fractions analyzed.

4.4. Sample DG122, unit 7, ~2200 m below the Monashee décollement

An intermediate structural level is represented by sample DG122, unit 7 pelitic schist, taken from a location within the overturned limb of the Sibley Creek syncline immediately proximal to the hinge (Fig. 4). The $^{208}Pb/^{232}Th$ ages, ranging from 61.8 ± 0.3 to 57.6 ± 0.2 Ma (Figs. 7a and 8), are substantially younger and more closely grouped at this locality than at higher structural levels and suggest a shorter duration of crystallization at a later time. Additionally, the U loss (~0.2–3.3%) for the fractions in this sample is interpreted to be minor at this level.

4.5. Sample DG167, unit 3, lowest structural level, ~3010 m below the Monashee décollement

Located within the lower, upright limb of the Sibley Creek syncline at the structurally lowest level sampled in this study, DG167 was taken from a pelitic schist of unit 3. The $^{208}Pb/^{232}Th$ ages are tightly clustered, ranging from 59.9 ± 0.3 to 59.4 ± 0.2 Ma, and are significantly younger than the ages produced at the highest structural levels. The data for this sample are interpreted to indicate a closed-system environment where crystallization of monazite was of short duration and U loss was insignificant (i.e. ~0.5–0.7%), suggesting a much simpler thermal history than at higher structural levels.

4.6. Age of the Sibley Creek syncline and its modification by F_2

The time of initiation of the Sibley Creek syncline and related F_1 structures is not well-constrained since these structures appear to have been initiated prior to peak-metamorphic conditions (Journeay, 1986; Scammell, 1986). Presumably the folding did not develop until some time after initial burial related to northeastward migration of the orogenic front. Palinspastic restoration and stratigraphic constraints in the Foreland Belt suggest that this did not occur before the Cretaceous (Price and Mountjoy, 1970; Brown et al., 1993). At outcrop scale, syn-peak-metamorphic F_2 structures penetratively overprinted the macroscopic-scale Sibley Creek syncline and, through ductile deformation, modified the pre-existing structure of the Sibley Creek syncline. Thus, the important constraints are the times at which the Sibley Creek syncline was modified by superposition of syn-peak-metamorphic F_2 structures. From the previous section it is apparent that this modification progressed from the upper limb to the lower limb over a minimum period of approximately 18–20 Ma in the Late Cretaceous to Paleocene.

5. Thermotectonic models

5.1. Apparent metamorphic age inversion

The monazite data are interpreted to reflect the timing of high temperature prograde metamorphism at each locality based on petrography which displays monazite crystals intergrown with the peak mineral assemblages (Fig. 9). Furthermore, the fact that all four pelitic localities exhibit the same general bulk composition and metamorphic assemblage indicates that the causes for monazite crystallization (i.e. heating and chemical reactions) were approximately the same

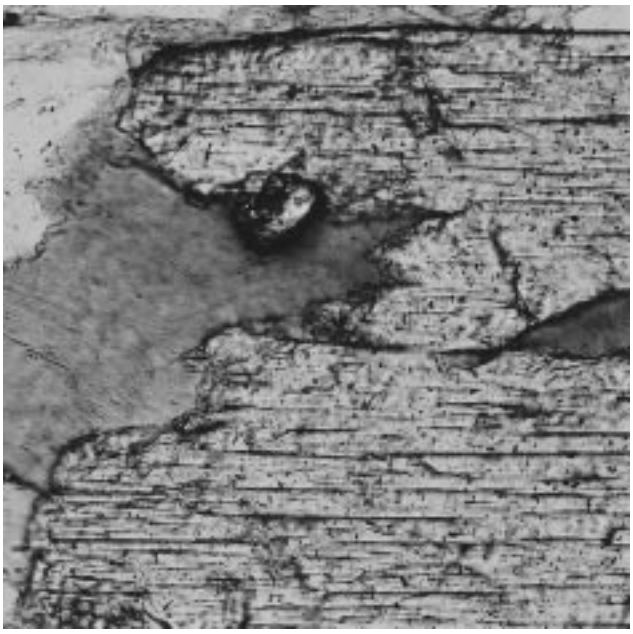

Fig. 9. Plain light photomicrograph of thin section from sample DG105 demonstrating textural relationship between a monazite crystal and the surrounding peak metamorphic mineral assemblage. The monazite crystal is located in the upper-mid section of the photograph (small, high relief crystal). The monazite grain boundaries are in contact with those of kyanite and biotite. This textural relationship is found in all the analyzed samples and is interpreted to indicate that the monazite grew approximately coeval with the peak metamorphic mineral assemblage (e.g. kyanite and biotite). Width of photomicrograph is 0.42 mm.

for each sample, regardless of structural level. Two cross-sections have been constructed at an acute angle to each other (Fig. 7a and b), which show the estimated position of the sample localities with respect to the Sibley Creek syncline and the projected position of the Monashee décollement. Additionally, Fig. 8 illustrates the relationship of monazite ages to depth below the Monashee décollement. From these figures, it is clear that the age of prograde metamorphism decreases with increasing structural depth. Accepting that the monazite ages represent the time of heating associated with prograde metamorphism for their respective structural levels, this age profile appears to be inverted compared to the expected distribution of prograde metamorphic ages for a normal, 'right-way-up' metamorphism in which age should increase with structural depth. This inversion is consistent with the results produced further south within the Monashee complex (Crowley, 1997; Crowley and Parrish, in press), where zircon, monazite, titanite, and hornblende ages illustrate a younging of peak thermal conditions at progressively lower structural levels beneath the Monashee décollement.

Another observed trend is the decrease in the spread of ages for each sample with increasing structural depth beneath the Monashee décollement (Fig. 8). The greatest range is found closest to the décollement (DG105, ~10 Ma), whereas the tightest clustering is found at the deepest structural level (DG167, ~0.5 Ma). This trend was also noted by Crowley (1997), who interpreted this to reflect a decreasing duration of peak thermal conditions at structurally deeper levels. Within the limits of this study and the data generated, there is not sufficient evidence to test this interpretation. Nevertheless, based on the observations made above one can conclude that monazites from rocks sampled closest to the Monashee décollement experienced a more protracted thermal history and grew at an earlier time than those located deeper in the tectonic pile.

5.2. Rapid Paleocene burial and Eocene denudation

Parrish (1995) argued that the Monashee complex was rapidly underthrust beneath the hot Selkirk allochthon during the Paleocene, causing a thermal inversion which resulted in an inverted Barrovian metamorphism. This was followed immediately by rapid exhumation of the complex and the allochthon during Eocene extension. Parrish based these conclusions on petrographic evidence presented by Journeay (1986) and on geochronologic data produced within and around the complex that suggested a brief thermal peak of 600–700°C at approximately 60–55 Ma.

5.3. Problems with the heat transfer model

The geochronologic and structural data presented in this study are incompatible with a model which proposes that the observed inverted metamorphic field gradient was the result of a crustal thermal inversion. The monazite $^{208}Pb/^{232}Th$ ages, which are considered to be the best approximation for the time of prograde metamorphism, are not consistent with rapid burial and heating of the complex initiating in the Paleocene. Monazite from sample DG105 began to crystallize by at least 77.7 ± 0.3 Ma, suggesting that elevated thermal conditions, presumably due to substantial tectonic burial beneath the overriding Selkirk allochthon (bathozone 5 of Carmichael, 1978, ca. 6.4–7.1 kbar or ~22–25 km depth; cf. Scammell, 1986), were reached prior to the Paleocene. Additionally, observations and interpretations presented herein suggest that rocks closest to the overlying heat source (Selkirk allochthon) were maintained at peak thermal conditions for at least 10 Ma. This prolonged duration of elevated temperatures is difficult to reconcile with model studies by England and Thompson (1984) and Ruppel and Hodges (1994), which indicate that a thermal inversion can only be sustained for a few million years. The long duration of elevated temperatures indicated by the

data should have allowed for nearly complete thermal relaxation of the isotherms, erasing any evidence of inverted isograds within the Monashee complex.

Another limitation of the thermal inversion model is that it does not consider the potential role played by deformation. Without invoking a significant component of mechanical modification, the distribution of ages found in this study is difficult to explain. There is at least an 18.3 Ma age difference between the initiation of monazite growth for the highest and lowest structural levels sampled (DG105 and DG167). If, as assumed, the initiation of growth was coeval with the timing of high-temperature prograde metamorphism at these levels, and the structural distance between the two levels was ~1.7 km (Figs. 7 and 8), then thermal inversion would require an extremely slow rate of conductively driven heat diffusion from the overlying allochthon. A first-order approximation of the vertical distance (Z) that would be penetrated in 18.3 Ma (t) by heat conducted from the overthrust Selkirk allochthon has been calculated using the following equation (modified from Oxburgh, 1981):

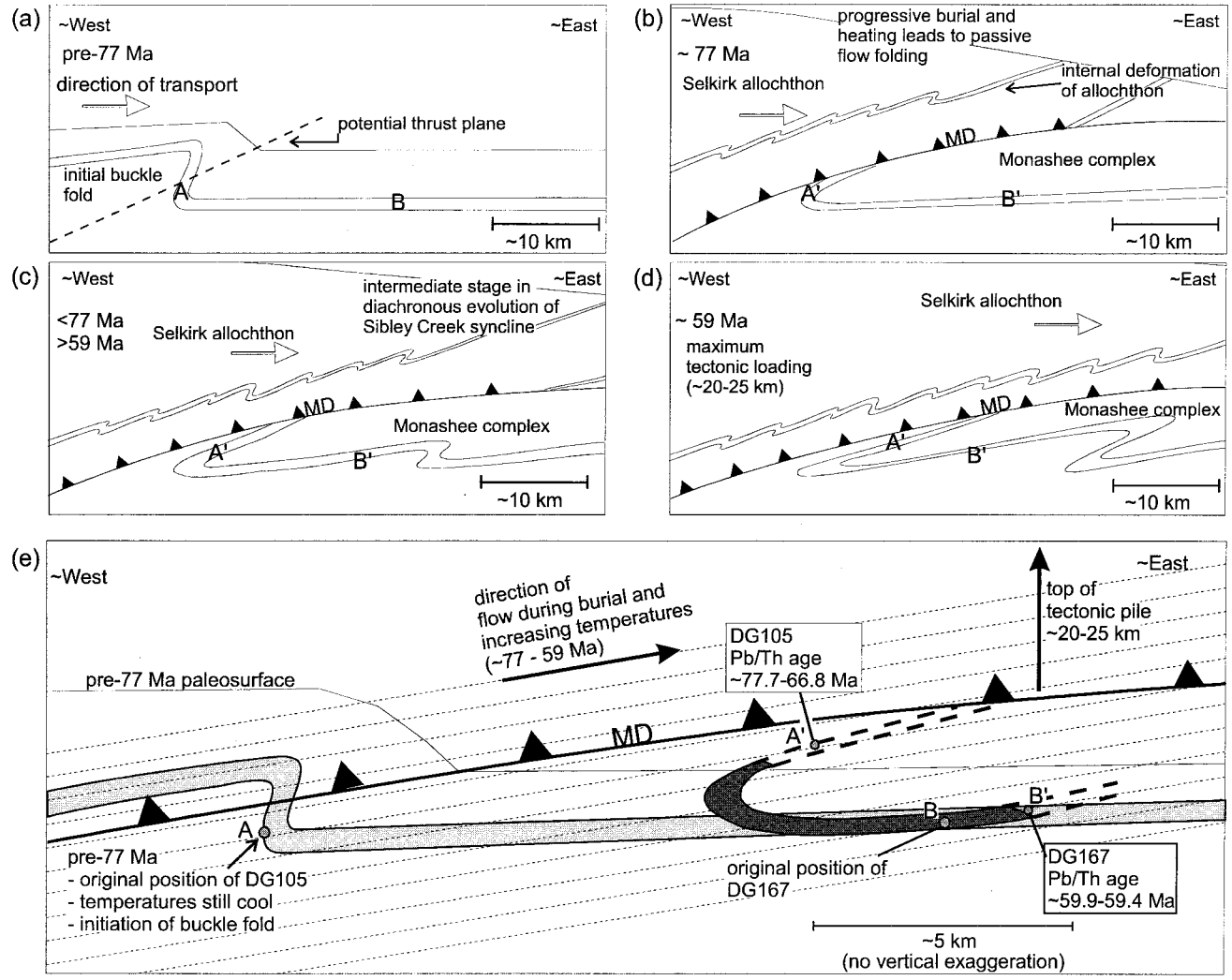

Fig. 10. Schematic thermotectonic model for northern Monashee complex; (a–d) illustrates the progressive burial and deformation of the Monashee complex with time. Cordilleran deformation and burial of the Monashee complex beneath the Selkirk allochthon is initiated prior to 77 Ma (a) and progresses diachronously until ca. 59 Ma (d) when the tectonic load is maximum (at a depth of ~20–25 km); extensional unloading immediately follows (Parrish et al., 1988 and references therein). The Sibley Creek syncline (SCS) originates prior to 77 Ma (a) as a buckle fold in a relatively cool environment but evolves into a thermally aided passive flow fold with increased heat and tectonic load (b–d). Rocks initially located to the west are buried and heated first (e.g. DG105 with minimum age range of ~77–67 Ma) and are laterally transported over rocks to the east, which reach peak temperatures and depths at a later time (~59 Ma). Based on the concepts proposed in the general model illustrated in (a–d), (e) incorporates a scaled cross-section of the Sibley Creek syncline and the flow lines of the rocks initially found to the west as they are transported eastward in a passive-flow fashion resulting in the present-day geometry of the Sibley Creek syncline and in the distribution of inverted and strongly diachronous peak-metamorphic ages.

$$Z = \sqrt{\kappa t} \quad (1)$$

where κ is thermal diffusivity in continental crust, which is estimated to be between $\sim 6.0 \times 10^{-7}\ m^2\ s^{-1}$ and $1.2 \times 10^{-6}\ m^2\ s^{-1}$ (England and Thompson, 1984). As a result, a vertical separation of ~18.6–26.3 km between the highest and lowest sample localities is required, equal to at least 10 times the actual observed distance. Additionally, the above calculation does not consider the heat input from radioactive decay within the thickened crust which would further increase the distance penetrated by conducted heat. Conversely, if it had taken 18.3 Ma for the heat to penetrate the restricted vertical distance of ~1.7 km, an inexplicably low heat diffusivity value of approximately $5.0 \times 10^{-9}\ m^2\ s^{-1}$ would be required. However, it should be noted that the present 1.7 km distance between the samples may be considered a minimum value of the original thickness and that deformation may have played a significant role in thinning the tectonic pile. These thermomechanical processes are considered below.

5.4. Conceptual thermomechanical model

Thermochronologic and structural data presented in this paper indicate that the Sibley Creek syncline, which began to develop prior to the onset of pre-peak-metamorphic conditions (F_1), was modified by diachronous penetrative syn-peak-metamorphic deformation (F_2) from approximately 78 to 59 Ma. At pre-peak conditions, the initiation of folding would have taken place when the rocks exhibited a high ductility contrast. Therefore, in the earliest stages the Sibley Creek syncline is presumed to have been an open fold with little or no limb attenuation (Fig. 10a). As the eastward advancing Selkirk allochthon buried the Monashee complex (Fig. 10b–d) the fold tightened and stratigraphy became transposed. Strong eastward vergent deformation placed more deeply buried western strata over less deeply buried eastern strata (Fig. 10a–e). Fig. 10(e) diagrammatically illustrates how rocks now found in the overturned limb of the Sibley Creek syncline may have been translated eastward. By way of example, point (A) is displaced 11 km from its initial position along passive flow lines at a rate of approximately $0.6\ mm\ y^{-1}$ for approximately 18 Ma, as suggested by the geochronologic constraints and the geometry of the syncline. Rocks located in the lower limb (B) travelled significantly smaller distances (B–B′ approximately 1.5 km) for a shorter period of time (possibly 0.5–1 Ma). Since the western parts of the fold were buried and heated earlier than the eastern parts, peak metamorphism developed first in the west and then migrated to the east; eastward vergent progressive deformation placed these western rocks over the eastern rocks as the fold evolved to its present geometry. This scenario would give rise to the presently preserved distribution of diachronous peak-metamorphic ages at the present time and to the inverted metamorphic field gradient. At approximately 59 Ma the Monashee complex was rapidly exhumed as normal-sense shearing on the Columbia River and Okanagan–Eagle River fault systems removed much of the crustal cover (Johnson and Brown, 1996 and references therein), thus facilitating rapid cooling of the complex and preservation of the inverted metamorphic field gradient and peak-metamorphic ages.

6. Discussion

To overcome the apparent difficulties in applying a simple thermal inversion scenario to explain the occurrence of an inverted metamorphic field gradient, the model presented above combines both thermal and mechanical processes; diachronous burial leads to diachronous peak metamorphism, and progressive deformation places the early peak-metamorphic rocks structurally above the late peak-metamorphic rocks. It is reasonable to assume that heat from the overlying Selkirk allochthon contributed to the heating of the underlying rocks, but this is not essential to the model and may have played an insignificant role. Accordingly, the role of local heating or cooling due to transmission of fluids during metamorphism is not discounted but is not considered to be a significant mechanism that would explain the systematic nature of the ~18.3 Ma decrease in age with the ~1.7 km increase in depth found in this study. Furthermore, the same consistently downward younging trend is found further south and deeper within the complex (Crowley, 1997; Crowley and Parrish, in press), adding at least another 3–4 km depth to the overall profile of ages and casting further doubt on fluid transmission as a significant mechanism for an inversion of metamorphic ages.

The deformation model, while serving to explain the thermochronologic data, is not intended to be an exact explanation of the structural kinematic history; it is recognized that the flow was most likely complex and three dimensional. For example, the F_2 structures are reclined and display strong regional northward vergence. A discussion of these complexities will be the subject for future communications.

The implications of this study beyond the regional context of the Monashee complex are worth consideration. For instance, in recent years several models have been proposed to explain the occurrence of an inverted metamorphic sequence in the Main Central thrust zone of the Himalayas (see Introduction). The model presented in this paper agrees well with models

that invert metamorphic field gradients via distributed ductile processes (e.g. Hubbard, 1996; Grujic et al., 1996; Jamieson et al., 1996) and casts further doubt on models that argue inversion was caused primarily by transmission of heat into the footwall from above. As such, conducting a detailed geochronologic analysis similar to the one carried out in this study may further elucidate the cause of inverted metamorphic field gradients observed in the Himalayas and in other orogens where this phenomenon occurs. Furthermore, although not attempted within the scope of this study, the results indicate that such detailed geochronologic studies could constrain the rate of development of structures within a middle crustal setting during orogenic processes.

7. Conclusions

The Sibley Creek syncline evolved over a period of at least 18–20 Ma, during which time it was significantly modified by syn-peak-metamorphic deformation (F_2); this deformation was initiated by at least ca. 77 Ma. The generations of deformation described in this paper are local markers of progressive deformation, but each evolved diachronously as a function of the advance of the orogenic front and resulting structural depth beneath the Selkirk allochthon. An analysis of the structure and geochronology of the area indicates that the pattern of dates relative to the overlying allochthon is consistent with distributed ductile deformation of isograd surfaces by substantial east-directed shear strain and attendant attenuation in the footwall, leading to relative lateral transfer of rocks preserving evidence of inverted diachronous metamorphism. Previous tectonic models of the region that attribute the distribution of diachronous and inverted peak-metamorphic assemblages solely to conductive heating from a hot overthrusted allochthon are rejected.

Acknowledgements

Fieldwork and U–Th–Pb laboratory procedures carried out by H.D. Gibson were supported by Geological Survey of Canada (GSC) and NSERC operating grants to R.R. Parrish and R.L. Brown, respectively. The work benefited greatly from discussions with Jim Crowley, Paul Williams, Dennis Johnston, and Sharon Carr. Rebecca Jamieson and Mary Hubbard are thanked for their constructive reviews which greatly improved this communication. Jesse Coburn is thanked for his field assistance. Lois Hardy is gratefully acknowledged for her editorial help with the manuscript.

References

Armstrong, R.L., Parrish, R.R., van der Heyden, P., Scott, K., Runkle, D., Brown, R.L., 1991. Early Proterozoic basement exposures in the southern Canadian Cordillera: core gneiss of Frenchman Cap, Unit 1 of the Grandforks Gneiss and the Vaseaux Formation. Canadian Journal of Earth Sciences 28, 1169–1201.

Barth, S., Oberli, F., Meier, M., 1994. Th–Pb versus U–Pb isotope systematics in allanite from co-genetic rhyolite and granodiorite: implications for geochronology. Earth and Planetary Science Letters 124, 149–159.

Bhattacharya, D.S., Das, K.K., 1983. Inversion of metamorphic zones in the lower Himalaya at Gangtok, Sikkim, India. Journal of Geology 91, 98–102.

Bordet, P., 1961. Recherches géologiques dans l'Himalaya du Népal, région du Makalu. Centre Nationale de Recherche Scientifique, Paris.

Brown, R.L., 1980. Frenchman Cap dome, Shuswap complex, British Columbia: a progress report. Geological Survey of Canada Paper 80-1A, 47–51.

Brown, R.L., Journeay, J.M., 1987. Tectonic denudation of the Shuswap metamorphic terrane of southeastern British Columbia. Geology 15, 142–146.

Brown, R.L., Psutka, J.F., 1979. Stratigraphy of the east flank of Frenchman Cap dome, Shuswap complex, British Columbia. Geological Survey of Canada Paper 79-1A, 35–36.

Brown, R.L., Journeay, J.M., Lane, L.S., Murphy, D.C., Rees, C.J., 1986. Obduction, backfolding and piggyback thrusting in the metamorphic hinterland of the southeastern Canadian Cordillera. Journal of Structural Geology 8, 255–268.

Brown, R.L., Carr, S.D., Johnson, B.J., Coleman, V.J., Cook, F.A., Varsek, J.L., 1992. The Monashee décollement of the southern Canadian Cordillera: a crustal-scale shear zone linking the Rocky Mountain Foreland Belt to lower crust beneath accreted terranes. In: McClay, K.R. (Ed.), Thrust Tectonics. Chapman and Hall, London, pp. 357–364.

Brown, R.L., Beaumont, C., Willett, S.D., 1993. Comparison of the Selkirk fan structure with mechanical models: Implications for interpretation of the southern Canadian Cordillera. Geology 21, 1015–1018.

Brunel, M., Kienast, J.R., 1986. Étude pétro-structurale des chevauchements ductiles himalayens sur la traversale de l'Everest–Makalu (Népal oriental). Canadian Journal of Earth Sciences 23, 1117–1137.

Carmichael, D.M., 1978. Metamorphic bathozones and bathograds: a measure of the depth of post-metamorphic uplift and erosion on the regional scale. American Journal of Science 278, 769–797.

Carr, S.D., 1991. Three crustal zones in the Thor–Odin–Pinnacles area, southern Omineca Belt, British Columbia. Canadian Journal of Earth Sciences 28, 2003–2023.

Cook, F.A., Varsek, J.L., Clowes, R.M., Kanasewich, E.R., Spencer, C.S., Parrish, R.R., Brown, R.L., Carr, S.D., Johnson, B.J., Price, R.A., 1992. Lithoprobe crustal reflection cross section of the southern Canadian Cordillera. 1. Foreland Thrust and Fold Belt to Fraser River fault. Tectonics 11, 12–25.

Crowley, J.L., 1997. U–Pb geochronology in Frenchman Cap dome of the Monashee complex, southern Canadian Cordillera; Early Tertiary tectonic overprint of a Proterozoic history. Unpublished Ph.D. Thesis, Carleton University, Ottawa, Ontario, Canada.

Crowley, J.L., 1999. U–Pb geochronologic constraints on Paleoproterozoic tectonism in the Monashee complex, Canadian Cordillera: elucidating an overprinted geologic history. Geological Society of America Bulletin 111, 560–577.

Crowley, J.L., Parrish, R.R., in press. U–Pb isotopic constraints on

diachronous metamorphism in the northern Monashee complex, southern Canadian Cordillera. Journal of Metamorphic Geology.

Dodson, M.H., 1973. Closure temperature in cooling geochronological and petrological systems. Contributions to Mineralogy and Petrology 40, 259–274.

England, P.C., Molnar, P., 1993. The interpretation of inverted metamorphic isograds using simple physical calculations. Tectonics 12, 145–157.

England, P.C., Thompson, A.B., 1984. Pressure–Temperature–Time paths of regional metamorphism I. Heat transfer during the evolution of regions of thickened continental crust. Journal of Petrology 25-4, 894–928.

Gibson, H.D., 1997. Thermotectonic evolution of the northern Monashee complex, southern Omineca Belt, southeastern British Columbia. Unpublished M.Sc. Thesis, Carleton University, Ottawa, Ontario, Canada.

Grujic, D., Casey, M., Davidson, C., Hollister, L., Kundig, R., Pavlis, T., Schmid, S., 1996. Ductile extrusion of the Higher Himalayan Crystalline in Bhutan: Evidence from quartz microfabrics. Tectonophysics 260, 21–43.

Höy, T., Brown, R.L., 1980. Geology of eastern margin of Frenchman Cap dome. British Columbia Ministry of Energy, Mines, and Petroleum Resources, Preliminary Map 43.

Hubbard, M.S., 1989. Thermobarometric constraints on the thermal history of the Main Central Thrust Zone and Tibetan Slab, eastern Nepal Himalaya. Journal of Metamorphic Geology 7, 19–30.

Hubbard, M.S., 1996. Ductile shear as a cause of inverted metamorphism: example from the Nepal Himalaya. Journal of Geology 104, 493–499.

Jamieson, R.A., 1986. P–T paths from high temperature shear zones beneath ophiolites. Journal of Metamorphic Geology 4, 3–22.

Jamieson, R.A., Beaumont, C., Hamilton, J., Fullsack, P., 1996. Tectonic assembly of inverted metamorphic sequences. Geology 24, 839–842.

Johnson, B.J., Brown, R.L., 1996. Crustal structure and Early Tertiary extensional tectonics of the Omineca Belt at 51°N latitude, southern Canadian Cordillera. Canadian Journal of Earth Sciences 33, 1596–1611.

Journeay, J.M., 1986. Stratigraphy, internal strain and thermotectonic evolution of northern Frenchman Cap dome: an exhumed duplex structure, Omineca hinterland, SE Canadian Cordillera. Unpublished Ph.D. thesis, Queen's University, Kingston, ON.

Journeay, J.M., Brown, R.L., 1986. Major tectonic boundaries of the Omineca Belt in southern British Columbia: a progress report. Geological Survey of Canada Paper 86-1A, 81–88.

Journeay, M., 1991. Geology of north central Frenchman Cap Dome Monashee terrane, southeast British Columbia. Geological Survey of Canada Open file 2447, scale 1:50 000.

Keppler, H., Wyllie, J., 1990. Role of fluids in transport and fractionation of uranium and thorium in magmatic processes. Nature 348, 531–533.

Kretz, R., 1983. Symbols for rock-forming minerals. American Mineralogist 68, 277–279.

Le Fort, P., 1975. Himalayas: the collided range. Present knowledge of the continental arc. American Journal of Science 275-A, 1–44.

Le Fort, P., 1986. Metamorphism and magmatism during the Himalayan collision. In: Coward, M.P., Ries, A.C. (Eds.), Collision Tectonics. Geological Society of London Special Publication, 19, pp. 159–172.

Oxburgh, E.R., 1981. Heat flow and magma genesis. In: Hargraves,, R.B. (Ed.), Physics of Magmatic Processes. Princeton University Press, Princeton, New Jersey, pp. 161–194 Chapter 5.

Parrish, R.R., 1995. Thermal evolution of the southeastern Canadian Cordillera. Canadian Journal of Earth Sciences 32, 1618–1642.

Parrish, R.R., Carr, S.D., Parkinson, D.L., 1988. Eocene extensional tectonics and geochronology of the southern Omineca Belt, British Columbia and Washington. Tectonics 7, 181–212.

Price, R.A., Mountjoy, E.W., 1970. Geologic structure of the Canadian Rocky Mountains between Bow and Athabasca Rivers—A progress report. In: Wheeler, J.O. (Ed.), Structure of the Southern Canadian Cordillera, 6. Geological Society of Canada Special Paper, pp. 7–25.

Psutka, J.F., 1978. Structural setting of the Downie Slide, northeast flank of Frenchman Cap gneiss dome, Shuswap Metamorphic complex, southeastern British Columbia. Unpublished M.Sc. thesis, Carleton University, Ottawa, Canada.

Ramsay, J.G., Huber, M.I., 1987. In: The Techniques of Modern Structural Geology, Volume 2: Folds and Fractures. Academic Press, London.

Read, P.B., Brown, R.L., 1981. Columbia River fault zone: southeastern margin of the Shuswap and Monashee complexes, southern British Columbia. Canadian Journal of Earth Sciences 18, 1127–1145.

Reddy, S.M., Searle, M.P., Massey, J.A., 1993. Structural evolution of the High Himalayan Gneiss sequence, Langtang Valley, Nepal. In: Treloar, P.J., Searle, M.P. (Eds.), Himalayan Tectonics, Geological Society of London Special Publication, 74, pp. 375–389.

Royden, L.H., 1993. The steady state thermal structure of eroding orogenic beltbelts and accretionary prisms. Journal of Geophysical Research 98, 4487–4507.

Ruppel, C., Hodges, K.V., 1994. Pressure–Temperature–Time paths from two-dimensional thermal models: prograde, retrograde, and inverted metamorphism. Tectonics 13, 17–44.

Scammell, R.J., 1986. Stratigraphy, structure and metamorphism of the north flank of the Monashee complex, southeastern British Columbia: a record of the Proterozoic crustal thickening. Unpublished M.Sc. thesis, Carleton University, Ottawa, Canada.

Scammell, R.J., Brown, R.L., 1990. Cover gneisses of the Monashee Terrane: a record of synsedimentary rifting in the North American Cordillera. Canadian Journal of Earth Sciences 27, 712–726.

Searle, M., Waters, D.J., Rex, A.J., Wilson, R.N., 1992. Pressure, temperature, and time constraints on Himalayan metamorphism from eastern Kashmir and western Zanskar. Geological Society of London Journal 149, 753–773.

Smith, H.A., Barreiro, B., 1990. Monazite U–Pb dating of staurolite grade metamorphism in pelitic schists. Contributions to Mineralogy and Petrology 105, 602–615.

Spear, F.S., 1993. Metamorphic Phase Equilibria and Pressure–Temperature–Time paths. Mineralogical Society of America Monograph, p. 799.

Spear, F.S., Parrish, R.R., 1996. Petrology and cooling rates of the Valhalla complex, British Columbia, Canada. Journal of Petrology 37, 733–765.

Tilley, C.E., 1925. Preliminary surveys of metamorphic zones in the southern Highlands of Scotland. Quarterly Journal of Geological Sciences 81, 100–112.

Treloar, P.J., Williams, M.P., Coward, M.P., 1989. Metamorphism and crustal stacking in the North India Plate, North Pakistan. Tectonophysics 165, 167–184.

Wheeler, J.O., 1965. Big Bend map-area, British Columbia. Geological Survey of Canada Paper 64-32, 1–37.

Wheeler, J.O., McFeely, P., 1991. Tectonic assemblage map of the Canadian Cordillera and adjacent parts of the United States of America. Geological Survey of Canada Map 1712A, scale 1:2 000 000.